CHAPTER III

THEORY

In the previous chapter, a review was given of recent research on alumina synthesis by solvothermal method, mixed-phase of alumina supports for supported cobalt catalysts, and alumina supports containing promoters or modifiers for supported iron catalysts. It provides knowledge and understanding of influencing parameters of alumina supports on the performance of Co and Fe catalysts for CO hydrogenation and FTS system. This chapter focuses on the fundamental theory of the Fischer-Tropsch Synthesis (FTS) which is well known as one type of carbon monoxide (CO) hydrogenation using Co and Fe catalysts. The chapter consists of eight main sections. Basic details of Fischer-Tropsch Synthesis (FTS) are discussed in section 3.1. Alumina which is used as the support is explained in section 3.2. Details of the solvothermal method are described in section 3.3. Cobalt and cobalt catalysts are discussed in section 3.4 and 3.5, respectively. Iron and iron catalysts are detailed in section 3.6 and 3.7, respectively. Details of Cu promoters for FTS are discussed in the last section 3.8.

3.1 Fischer-Tropsch synthesis (FTS)

Fischer-Tropsch synthesis (FTS), first developed in Germany in 1923, is an alternate process in the production of liquid fuels and chemicals from synthesis gas (H_2/CO) derived from coal, natural gas, and other carbon-containing materials such as peat, and biomass (Zhang *et al.*, 2006). Normally, the FTS product consists of a complex multicomponent mixture of linear and branched hydrocarbons and oxygenated products. Main products are linear paraffins and a-olefins (Van der laan and Beenackers, 1999). Fuels produced with the FTS compared to crude oil as a feedstock for fuel production are of a high quality due to a very low aromaticity and zero sulfur content. The kerosene/jet fuel produced has good combustion properties and high smoke points and the diesel fuel with its high cetane number can be used to upgrade lower quality blend stocks produced from crude oil. Linear olefins required

in the chemical industry can be produced either directly in the FTS process (Steynberg and Dry, 2004). During the past decades, FTS has been developed continuously by many researchers, although the rise and fall in research intensity on this process has been highly related to the demands for liquid fuels and relative economics.

This synthesis is basically the reductive polymerization (oligomerization) of carbon monoxide by hydrogen to form organic products containing mainly hydrocarbons and some oxygenated products in lesser amounts. The main reactions of FTS are:

$$CO + \left(1 + \frac{m}{2n}\right)H_2 \rightarrow \left(\frac{1}{n}\right)C_nH_m + H_2O \quad (1)$$

$$CO + 3H_2 \rightarrow CH_4 + H_2O \quad (2)$$

$$CO + H_2O \rightarrow CO_2 + H_2 \quad (3)$$

$$2CO \rightarrow C + CO_2 \quad (4)$$

Equations (1) is the formation of hydrocarbons higher than C1, and the equation (2) is methanation. The water-gas shift reaction, which is undesirable for natural gas conversion, is shown in equation (3). The Boudouard reaction, which results in carbon deposition on the catalyst surface, is shown in equation (4).

The mechanism consists of surface steps in five categories: (1) the adsorption of reactants (H_2 and CO); (2) chain initiation; (3) chain propagation; (4) chain termination and desorption of products; (5) readsorption and secondary reaction of olefins. Depending upon the type of catalyst used, promoters, reaction conditions (pressure, temperature and H_2/CO ratios), and type of reactors, the distribution of the molecular weight of the hydrocarbon products can be noticeably varied. The following set of mechanism below described the reaction mechanism of methanation.

(1) CO + * = CO*

(2) CO* + * = C* +O*

(3) $H_2 + 2^* = 2H^*$

(4) $C^* + H^* = CH^* + *$

(5) $CH^* + H^* = CH_2^* + *$

(6) $CH_2^* + H^* = CH_3^* + *$

(7) $CH_3^* + H^* = CH_4(g) + 2^*$

(8) $O^* + H^* = OH^* + *$

(9) $OH^* + H^* = H_2O(g) + 2^*$

Normally, catalysts used for FTS are group VIII metals. By nature, the hydrogenation activity increases in order of Fe < Co < Ni < Ru. Ru is the most active. Ni forms predominantly methane, while Co yields much higher ratios of paraffins to olefins and much less oxygenated products such as alcohols and aldehydes than Fe does.

With regards to the operating conditions, usually higher pressures will result in higher rates. There are basically three reactor types used for FTS: (1) fixed bed, (2) fluid bed, and (3) slurry bed. Because of the high exothermicity of the reaction (142 kJ mol^{-1} of reacted carbon), all three reactor types are carefully designed for rapid heat removal using a combination of various techniques including heat exchange, recycle, fluidized and slurry beds, and stage systems. The attributes, advantages and limitations of each of these reactors is different as summarized below.

Fixed-bed reactor: In a typical fixed bed reactor heat is removed by heat exchangers or by production of steam. To facilitate temperature control while maximizing conversion and linear gas velocity, a portion of the tail gas is recycled, typically with a recycle: fresh volume ratio of about 2. Since the heat exchanger design favors lower temperatures of operation (220-250°C), predominantly higher hydrocarbons including gasoline, diesel fuel and waxes are produced. *Fluid-bed reactors*: Fluid beds are of generally two types, fixed and circulating. This reactor has better heat removal (near isothermal operation), higher reaction temperature (exit temperature of 340°C) and hence higher selectivities for lighter products, alkenes, branched products and aromatics, and higher throughput per volume of reactor relative to the fixed bed. With on-line catalyst removal and addition, process runs are

much longer than for the fixed bed. Nevertheless, the fluid-bed reactor is a more complex system requiring an attrition-resistant catalyst and grater system maintenance. Moreover, process conditions and temperature must be adjusted to limit production of heavy hydrocarbons which would condense on the catalyst and defluidize the bed. *Slurry-bed reactor*: slurry-bed reactor, in which a finely divided catalyst is suspended in a heavy oil by gas bubbling up through the slurry, have been investigated fairly for FTS by Koelber, Sasol and Rheinpreussen-Koppers. This reactor type has the advantages of (1) capability of operating at low H_2:CO ratios without problems with carbon deposition, (2) very efficient heat transfer and uniform temperature, (3) high catalyst efficiency/performance, and (4) simple construction. Although some of the operating problems in using slurry bed reactor FTS are daunting, such as high slurry viscosities, particle settling, catalyst liquid-separation and possible gas-liquid mass transport limitations. Slurry-bed reactors are better than fixed-bed reactors for FTS since they can remove heat from this exothermic synthesis, allowing better temperature control.

The current main goal in FTS is to obtain high molecular weight, straight chain hydrocarbons. However, methane and other light hydrocarbons are always present as less desirable products from the synthesis. According to the Anderson-Schulz-Flory (ASF) product distribution, typically 10 to 20% of products from the synthesis are usually light hydrocarbon (C_1-C_4). These light alkanes have low boiling points and exist in the gas phase at room temperature, which is inconvenient for transportation. Many attempts have been made to minimize these by-products and increase the yield of long chain liquid hydrocarbons by improving chain growth probability. It would be more efficient to be able to convert these less desirable products into more useful forms, rather than re-reforming them into syngas and recycling them (Farrauto and Bartholomew, 1997). Depending upon the type of catalyst used, promoters, reaction conditions (pressure, temperature and H_2/CO ratios), and type of reactors, the distribution of the molecular weight of the hydrocarbon products can be noticeably varied.

3.2 Alumina (Al_2O_3)

Study of alumina has been a subject of great interest for many decades. Alumina is a very interesting crystalline material with broad applicability as adsorbents, coatings, soft abrasives, ceramic tools, fillers, wear-resistant ceramics, catalysts, and catalyst supports (Pajonk and Teichner, 1986; Church *et al.*, 1993). Because of their fine particle size, high surface area, high melting point (above 2000°C), high purity, good adsorbent, and high catalytic activity, they have been employed in a wide range of large-scale technological processes (Misra, 1986). The basic knowledge of alumina including the structure and phase transformation sequences of transition alumina is shown in this part.

3.2.1 The structure of alumina

1) Structure of Al_2O_3 polymorphs based on face-centered cubic packing of oxygen anions

Al_2O_3 polymorphs based on fcc packing of oxygen are represented by eight X-ray powder diffraction files, which are based on the experiments performed 30-40 years ago. These files described structures denoted γ-, η-, δ-, and θ-phase with a few additional files in which the same phase notation is used for similar but not identical profiles.

a) Cubic, spinel-type alumina: γ- and η-Al_2O_3

γ- and η-Al_2O_3 have been described as defect spinel structure (Perego and Villa, 1994). The ideal spinel structure AB_2O_4 is represented by 2×2×2 array of an fcc closet packing, with A and B cations occupying the 8*a* (of the 64 available) tetrahedrally and the 16*d* (of 32) octahedrally coordinated interstitial sites (Fig 3.1). The symmetry of the spinel structure is described by the $Fd\bar{3}m$ space group (Hahn, 1995). The packing of the {111} oxygen layers forms an ABCABC sequence, whereas the packing of aluminum cations can be described by two type of alternating layers: either (i) layer containing only octahedrally coordinated cations or (ii) "mixed"

layer containing both octahedrally and tetrahedrally coordinated cations. There are two types of tetrahedrally coordinated sites: upward and downward.

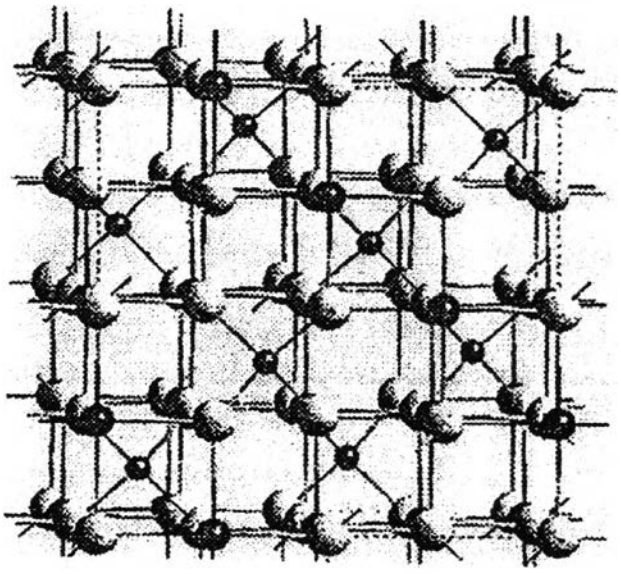

Figure 3.1 Three dimensional view of the spinel structure: White balls represent oxygen ions located at 32*e* Wyckoff positions. Large dark balls represent oxygen ions located at 16*d*, the smaller one represent 8*a*.

The commonly accepted structure model of γ-Al_2O_3 is related to that of ideal spinel and it is assumed to contain oxygen ions at 32*e* Wyckoff positions, which are approximately close packed, while 64/3 aluminum cations (to satisfy Al_2O_3 stoichiometry) are distributed over 16*d* octahedral and 8*a* tetrahedral sites (Hahn, 1995). In γ-Al_2O_3 8/3 aluminum vacancies have been assumed in random distribution over the tetrahedral sites (Wilson, 1979). Therefore the cation sublattice is partially disordered, comparing with the ideal spinel. Despite this disorder, the symmetry relations between the equivalent cation positions remain $Fd\bar{3}m$.

Shirasuka et al. (Shirasuka *et al.*, 1976) proposed that 62% of aluminum ions occupy 16-fold (16*c* and 16*d*) octahedral sites and assumed that the remaining aluminum ions distributed equally over the eightfold and the 48-fold tetrahedral sites. These results were confirmed by John et al. (John *et al.*, 1983), who deduced that 62% of aluminum ions were in octahedral sites in η-Al_2O_3 according to the results from

solid-state nuclear magnetic resonance (NMR). Recently, Zhou and Snyder (Zhou and Synder, 1991) have applied Rietveld analysis of neutron diffraction profiles for the structure refinement of both γ- and η- structures. They have suggested that the presence of aluminum is in abnormally coordinated 32*e* sites in the surface layers of the both phases, but with no aluminum cations on the eight fold, tetrahedral coordinated sites in η-Al_2O_3, in contradiction to the result by Shirasuka et al. However, the Zhou and Snyder interpretation seems reasonable, because it is consistent with molecule dynamic simulations of γ-Al_2O_3 surface (Ernst *et al.*, 1991). However, it is not clear how these results which are associated with the influence of surface ions are related to the bulk structure.

γ-Al_2O_3 obtained from thermal oxidation of aluminum containing alloys, by annealing of amorphous anodic Al_2O_3 films, or by plasma spraying shows preferred orientation (crystalline texture), with both $<100>_\gamma$ and $<110>_\gamma$ direction preferentially oriented parallel to the surface normal (Blonski and Garofalini, 1993). Recent molecular dynamic simulations of the surface structure of γ-Al_2O_3, which have included the non-integer number of cations in the unit cell, result in the following relation between the surface energies: $\gamma_{\{001\}} < \gamma_{\{111\}} < \gamma_{\{110\}}$ (Ernst *et al.*, 1991). These results are consistent with a {100} preferential orientation. These calculations indicate that the surface energies of γ-Al_2O_3 are much lower than those for α-Al_2O_3 which is consistent with high specific surface area of γ-Al_2O_3.

γ-Al_2O_3 developed by crystallization of anodic Al_2O_3 films or by thermal oxidation of aluminum and NiAl, contains a high density of {111} growth twins. These twins have been related to the platelike morphology of oxide scales (Doychak *et al.*, 1989) developed on the surface of NiAl during transient stages of thermal oxidation.

b) Al_2O_3 structures with tetragonal-orthorhombic symmetry: δ-Al_2O_3

δ-Al_2O_3 has been described as a superlattice of the spinel structure with ordered cation vacancies. The δ supercell has been confirmed to be a tripled unit cell of spinel with 160 ions per cell. Two possible unit cells have been suggested based on

X-ray and SAD: either tetragonal with $a_\delta = b_\delta = a_\gamma$ and $c_\delta = 3a_\gamma$ (Androff *et al.*, 1997) or orthorhombic with $a_\delta = a_\gamma$, $b_\delta = 1.5a_\gamma$ and $c_\delta = 2a_\gamma$ (Bonevich and Marks, 1992).

In all reports of the tetragonal δ unit cell, the structure has been derived from boehmite, whereas the orthorhombic δ unit cell has been observed for precursors obtained by quenching the melt or by thermal oxidation. It is not clear whether either structure exist or the tetragonal structure is a misinterpretation of the experimental data. The SAD results available on the orthorhombic δ-Al_2O_3 structure provide convincing evidence for the existence of this polymorph (Jayaram and Levi, 1989), whereas X-ray data ascribed the tetragonal unit cell also could have been derived from orthorhombic unit cell (Kohn *et al.*, 1957).

Jayaram and Levi (Jayaram and Levi, 1989) have studied orthorhombic δ-Al_2O_3 by TEM. Convergent-beam electron diffraction (CBED) has been used to determine the space group and $P2_12_12_1$ has been suggested.

c) Al_2O_3 structures with monoclinic symmetry: θ, θ″, λ, and θ′ Al_2O_3

The most studied Al_2O_3 polymorph with monoclinic symmetry is θ-Al_2O_3. This structure has the space group *C2/m* and contains 20 ions, with the aluminum cations equally distributes over octahedral and tetrahedral sites. In many reports, θ-Al_2O_3 has been reported to be multiple twined, preliminary on the (001) plane (Kohn *et al.*, 1957). Although the true symmetry of θ-Al_2O_3 has been determined to be monoclinic, this phase may also appear as orthorhombic due to polysynthetic twinning.

The existence of three additional monoclinic Al_2O_3 structure has been reported (Levin and Brandon, 1998). λ-Al_2O_3 has been observed in both plasma sprayed Al_2O_3 and thermally oxidizied aluminum. θ′-Al_2O_3 has been found in annealed anodic Al_2O_3 films, and θ″-Al_2O_3 has been found in the plasma-sprayed Al_2O_3. Based on these results, all four monoclinic phase (θ-,θ″-, λ-, and θ′-Al_2O_3) are assumed to evolve from γ-Al_2O_3 by cation ordering on the interstitial sites of the oxygen subcell, which remains approximately undisturbed by these transformations. The lattice parameters

and space groups of these four monoclinic Al_2O_3 phases, respected on γ-Al_2O_3 are summarized in Table 3.1.

Table 3.1 Metastable Al_2O_3 structures based on fcc packing oxygen anions (Levin and Brandon, 1998).

Phase	Lattice parameters	Space group	Cations/ unitcell	Orientation relationship with respect to γ-Al_2O_3
γ-Al_2O_3, η-Al_2O_3	$a_\gamma \approx 7.9$ Å	$Fd3m$	64/3	
θ-Al_2O_3	$a \approx 1.5a_\gamma$ $b = a_\gamma\sqrt{2}/4$ $c = a_\gamma\sqrt{2}/2$ $\beta = 104°$	$C2/m$	8	$(100)_\theta \parallel (001)_\gamma$ $[010]_\theta \parallel [110]_\gamma$
θ''-Al_2O_3	$a \approx 1.5a_\gamma$ $b = a_\gamma\sqrt{2}$ $c = a_\gamma\sqrt{2}$ $\beta = 104°$	$A12/n1'$	64	$(100)_{\theta''} \parallel (001)_\gamma$ $[010]_{\theta''} \parallel [110]_\gamma$
θ'-Al_2O_3	$a \approx a_\gamma\sqrt{3}/2$ $b \approx a_\gamma\sqrt{2}$ $c \approx a_\gamma\sqrt{2}$ $\beta \approx 94°$	$C2/m$	16	$(010)_{\theta'} \parallel (110)_\gamma$ $[100]_{\theta'} \parallel [112]_\gamma$
λ-Al_2O_3	$a \approx 3\sqrt{2}a_\gamma/2$ $b \approx 2a_\gamma$ $c \approx 1.5a_\gamma$ $\beta = 115°$	$P2_1/c$	64	$[010]_\lambda \parallel [100]_\gamma$ $(100)_\lambda \parallel (013)_\gamma$
δ-Al_2O_3	$a \approx a_\gamma$ $b \approx 2a_\gamma$ $c \approx 1.5a_\gamma$	$P2_12_12_1$	64	$[100]_\delta \parallel [001]_\gamma$ $(100)_\delta \parallel (100)_\gamma$
δ'-Al_2O_3	$a \approx a_\gamma$ $c \approx 3a_\gamma$	$P4_1$	64	$[001]_{\delta'} \parallel [001]_\gamma$ $(100)_{\delta'} \parallel (100)_\gamma$

2) Structure of Al_2O_3 polymorphs based on hexagonal close packing of oxygen anions

The common metastable Al_2O_3 crystal structures based on hcp close packing of the oxygen atom are κ- and χ-Al_2O_3. The existence of κ′-Al_2O_3 from the dehydration of tohdite has also been reported.

The partial transformation of gibbsite into boehmite, which gives its own dehydration products upon further heating, greatly complicates the interpretation of X-ray measurements for the structure of κ- and χ-Al_2O_3. Three different unit cells have been proposed. Stumpth et al. (Stumpf *et al.*, 1950) suggest that χ-alumina has a cubic (not spinel) unit cell of lattice parameter 7.95 Å, whereas other researchers (Brindley and Choe, 1961) propose hexagonal unit cells with either a = 5.56 Å and c = 13.44 Å or a = 5.57 Å and c = 8.64 Å. Hexagonal χ-alumina seems to possess a layer structure, the arrangement of anions being inherited from gibbsite, whereas the aluminum cations occupy octahedral sites with in the hexagonal oxygen layers. The stacking of the layers are strongly disordered in the c-direction. It is not yet clear whether all three of the above structures exist, or whether the differences among them are merely a matter of interpretation.

κ′-Al_2O_3 has been described in terms of the hcp packing of oxygen anions (inherited from tohdite), with the random distribution of cations over both tetrahedrally and octahedrally coordinated positions. This polymorph is considered to be a transient phase in the transformation to tohdite to κ-Al_2O_3.

The structure of κ-Al_2O_3, which is considered important in the chemical vapor deposition (CVD) technology, had been believed for many years to be hexagonal (Brindley and Choe, 1961). However, a recent lattice image studied by Liu and Skogsmo (Liu and Skogsmo, 1991) combined with CBED, shows that the true symmetry for this structure is orthorhombic. The pseudohexagonal symmetry then results from the coexistence of three twin-related orthorhombic variants rotated by 120° with respect to one another. The space group of κ-Al_2O_3 is $Pna2_1$, and the lattice

parameters are a = 4.69 Å, b = 8.18 Å and c = 8.87 Å. The proposed unit cell composes of 16 cations that are ordered on both tetrahedrally and octahedrally sites.

3) Structure of α-Al_2O_3

α-Al_2O_3 posses trigonal symmetry with rhombohedral Bravis centering (space group $R\text{-}\bar{3}c$) and has 10 atoms in the unit cell. The crystallography of α-Al_2O_3 has been discussed in detail by Kronberg (Kronberg, 1957) and Bilde-Sorensen et al. (Bilde-Sorensen *et al.*, 1996). The structure of α-Al_2O_3 can be considered as an hcp sublattice of oxygen anions, with 2/3 of the octahedral interstices filled with aluminum cations in an ordered array. This simplified model describes the nature of the ion packing but is somewhat misleading, because it does not reflect true trigonal symmetry of the crystal. One consequence of the trigonal symmetry is the nonequivalence of cation layer translation along the $[10\bar{1}0]$ and $[\bar{1}010]$ directions (using hexagonal indices), which has important implications for both basal slip and basal twinning in α-Al_2O_3, as discussed by Kaplan et al. (Kaplan *et al.*, 1995) and Pirouz et al. (Pirouz *et al.*, 1996). (In some cases this nonequivalence has been attributed incorrectly to the lack of an inversion center in α-Al_2O_3, which would be inconsistent with a-$\bar{3}$ centrosymmetric point group.)

The oxygen anions in α-Al_2O_3 occupy 18c Wyckoff positions (in the hexagonal description) with coordinates x,0,1/4 (x = 0.306), whereas the aluminum cations are located at 12c positions with coordinates 0,0,z (z = 0.347). Both x and z values deviate from the ideal value of 1/3, which would correspond to the atomic positions in the ideal close-packed structure. The aluminum cations are displaced along the [0001] direction toward the neighboring empty octahedral sites, resulting in a "puckering" of the cation layers. The cation displacements are accompanied by distortion of the oxygen sublattice. The hexagonal parameters for α-Al_2O_3, are c = 1.297 nm and a = 0.475 nm, with c/a = 2.73 nm and corresponds to six oxygen layers along the c-axis of the unit cell. For the oxygen sublattice alone (three oxygen layers), c/a = 1.58, slightly smaller than the ideal value of 1.63 associated with a hard-sphere model.

3.2.2 Phase transformation

Alumina can exist in many metastable phases before transforming to the stable α-alumina (corundum form). There are six principal metastable phases of alumina designated by the Greek letters chi (χ), kappa (κ), eta (η), theta (θ), delta (δ), and gamma (γ), respectively. Although the range of temperature in which each transition phase is thermodynamically stable has been reported by many researchers, it depends upon various factors such as degree of crystallinity of sample, amount of impurities in the starting materials, and thermal history of sample. Most of the studies on phase transformation of alumina were conducted by calcinations of alumina precursor. It was found that difference in the phase transformation sequence is resulted from the difference in the precursor structure (Wilson, 1979; Lippens and Boer, 1964). Moreover, the transformation sequence is irreversible. The nature of the product obtained by calcination depends on the starting hydroxide and on the calcination condition.

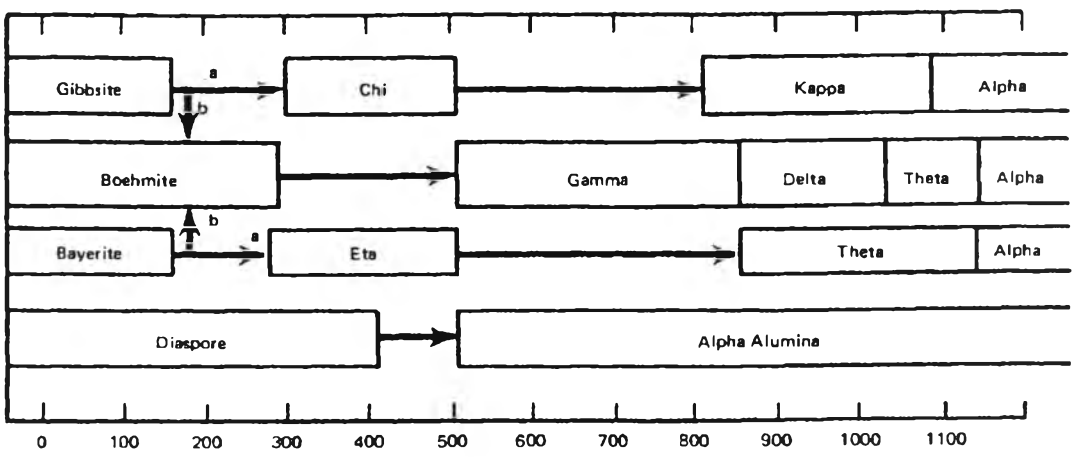

Figure 3.2 Decomposition sequence of aluminum hydroxides (Gitzen, 1970).

The phase transformation sequence normally starts with aluminum hydroxide ($Al(OH)_3$ and AlOOH) transforming to low-temperature phase of alumina (η and χ) at temperature around 150-500°C, and subsequently to high temperature phase (δ, θ, κ) at temperature around 650-1000°C. Finally, the thermodynamically stable phase, α-alumina, is formed at temperature around 1100-1200°C. It is generally believed that α-phase transformation takes place through the nucleation and growth mechanism.

Normally, transition alumina start to lose their surface area even at temperatures below 800°C due to the elimination of micro-pores. However, drastic loss occurs at temperatures higher than 1000°C when the crystallization to the thermodynamically stable α-alumina occurs (Dynys and Halloran, 1982).

3.3 Solvothermal method

Solvothermal synthesis is improved from the hydrothermal synthesis by using organic solvent as the reaction medium instead of water. This method is based on the decomposition of metal alkoxide at elevated temperature (200-300°C) under autogenous pressure. It is particularly suited for the synthesis of alumina in phase that is unstable at high temperature. It is also a useful technique for growing single crystals. In this method, parts or all of the reactants can dissolve in the organic solvent under high pressure. This feature enables the reaction to take place at lower temperature.

Generally, solvothermal equipment is basically a tube, usually made of steel, closed at one end. The other end has a screw cap with a gasket of soft copper to provide a seal. Alternatively, the "bomb" may be connected directly to an independent pressure source, such as a hydraulic ram. This is known as the "cold seal" method. The reaction mixture with appropriate amount of solvent are placed inside the bomb, which is then sealed and placed inside an oven at the required temperature, in the range of 100-500°C. Pressure is controlled either externally or by the degree of filling in the sealed bomb.

3.4 Cobalt (Young, 1960; Othmer, 1991)

3.4.1 General

Cobalt, a transition series metallic element having atomic number 27, is similar to silver in appearance.

Cobalt and cobalt compounds have expanded from use as colorants in glasses and ground coat frits for pottery to drying agents in paints and lacquers, animal and human nutrients, electroplating materials, high temperature alloys, hard facing alloys, high speed tools, magnetic alloys, alloys used for prosthetics, and used in radiology. Cobalt is also as a catalyst for hydrocarbon refining from crude oil for the synthesis of heating fuel.

3.4.2 Physical Properties

The electronic structure of cobalt is [Ar] $3d^7 4s^2$. At room temperature the crystalline structure of the α (or ε) form, is close-packed hexagonal (cph) and lattice parameters are a = 0.2501 nm and c = 0.4066 nm. Above approximately 417°C, a face-centered cubic (fcc) allotrope, the γ (or β) form, having a lattice parameter a = 0.3544 nm, becomes the stable crystalline form. Physical properties of cobalt are listed in Table 3.2.

The scale formed on unalloyed cobalt during exposure to air or oxygen at high temperature is double-layered. In the range of 300 to 900°C, the scale consists of a thin layer of mixed cobalt oxide, Co_3O_4, on the outside and cobalt (II) oxide, CoO, layer next to metal. Cobalt (III) oxide, Co_2O_3, may be formed at temperatures below 300 °C. Above 900°C, Co_3O_4 decomposes and both layers, although of different appearance, are composed of CoO only. Scales formed below 600°C and above 750°C appear to be stable to cracking on cooling, whereas those produced at 600-750°C crack and flake off the surface.

Cobalt forms numerous compounds and complexes of industrial importance. Cobalt, atomic weight 58.933, is one of the three members of the first transition series of Group 9 (VIIIB). There are thirteen know isotopes, but only three are significant: ^{59}Co is the only stable and naturally occurring isotope; ^{60}Co has a half-life of 5.3 years and is a common source of γ-radioactivity; and ^{57}Co has a 270-d half-life and provides the γ-source for Mössbauer spectroscopy.

Cobalt exists in the +2 or +3 valance states for the major of its compounds and complexes. A multitude of complexes of the cobalt (III) ion exists, but few stable simple salt are known. Octahedral stereochemistries are the most common for cobalt (II) ion as well as for cobalt (III). Cobalt (II) forms numerous simple compounds and complexes, most of which are octahedral or tetrahedral in nature; cobalt (II) forms more tetrahedral complex than other transition-metal ions. Because of the small stability difference between octahedral and tetrahedral complexes of cobalt (II), both can be found equilibrium for a number of complexes. Typically, octahedral cobalt (II) salts and complexes are pink to brownish red; most of the tetrahedral Co (II) species are blue.

Table 3.2 Physical properties of cobalt (Othmer, 1991).

Property	Value
atomic number	27
atomic weight	58.93
transformation temperature, °C	417
heat of transformation, J/g[a]	251
melting point, °C	1493
latent heat of fusion, ΔH_{fus} J/g[a]	395
boiling point, °C	3100
latent heat of vaporization at bp, ΔH_{vap} kJ/g[a]	6276
specific heat, J/(g °C)[a]	
15-100°C	0.442
molten metal	0.560
coefficient of thermalexpansion, $°C^{-1}$	
cph at room temperature	12.5
fcc at 417°C	14.2
thermal conductivity at 25°C, W/(m K)	69.16
thermal neutron absorption, Bohr atom	34.8
resistivity, at 20°C[b], $10^{-8}\Omega$ m	6.24
Curie temperature, °C	1121

Table 3.2 Physical properties of cobalt (cont.).

Property		Value	
saturation induction, $4\pi I_s$, T[c]		1.870	
permeability, μ			
initial		68	
max		245	
residual induction, T[c]		0.490	
coercive force, A/m		708	
Young's modulus, Gpac		211	
Poisson's ratio		0.32	
Hardness[f], diamond pyramid, of %Co		99.9	99.98[e]
At 20°C		225	253
At 300°C		141	145
At 600°C		62	43
At 900°C		22	17
strength of 99.99 %cobalt, MPa[g]	as cast	annealed	sintered
tensile	237	588	679
tensile yield	138	193	302
compressive	841	808	
compressive yield	291	387	

[a] To convert J to cal, divided by 4.184.

[b] conductivity = 27.6 % of International Annealed Copper Standard.

[c] To convert T to gauss, multiply by 10^4.

[d] To convert GPa to psi , multiply by 145,000.

[e] Zone refined.

[f] Vickers.

[g] To convert MPa to psi , multiply by 145.

3.4.3 Cobalt Oxides

Cobalt has three well-known oxides:

Cobalt (II) oxide, CoO, is an olive green, cubic crystalline material. Cobalt (II) oxide is the final product formed when the carbonate or the other oxides are calcined to a sufficiently high temperature, preferably in a neutral or slightly reducing atmosphere. Pure cobalt (II) oxide is a difficult substance to prepare, since it readily takes up oxygen even at room temperature to re-form a higher oxide. Above about 850°C, cobalt (II) oxide form is the stable oxide. The product of commerce is usually dark gray and contains 75-78 wt % cobalt. Cobalt (II) oxide is soluble in water, ammonia solution, and organic solvents, but dissolves in strong mineral acids. It is used in glass decorating and coloring and is a precursor for the production of cobalt chemical.

Cobalt (III) oxide, Co_2O_3, is formed when cobalt compounds are heated at a low temperature in the presence of an excess of air. Some authorities told that cobalt (III) oxide exists only in the hydrate form. The lower hydrate may be made as a black power by oxidizing neutral cobalt solutions with substances like sodium hypochlorite. Co_2O_3 or Co_2O_3. H_2O is completely converted to Co_3O_4 at temperatures above 265°C. Co_3O_4 will absorb oxygen in a sufficient quantity to correspond to the higher oxide Co_2O_3.

Cobalt oxide, Co_3O_4, is formed when cobalt compounds, such as the cabonate or the hydrated sesquioxide, are heated in air at temperatures above approximately 265°C and not exceeding 800°C.

3.5 Cobalt catalysts

Cobalt (Co) catalysts are the preferred catalysts for the synthesis of heavy hydrocarbons from natural gas based syngas (CO and H_2) because of their high Fischer-Tropsch (FT) activity, high selectivity for linear hydrocarbons, and low activity for the water gas shift reaction (Goellner and Gates, 2001). Generally, Co is deposited over an oxidic support, for example, SiO_2, Al_2O_3, ZrO_2, CeO_2 or TiO_2,

which provides good mechanical strength and thermal stability under reaction conditions (Iglesia, 1997). It is known that reduced cobalt metal, rather than its oxides or carbides, is the most active phase for CO hydrogenation in such catalysts. Investigations have been done to determine the nature of cobalt species on various supports such as alumina, silica, titania, zirconia, carbon, and zeolites. The influence of various types of cobalt precursors used was also investigated. It was found that the used of organic precursors such as CO (III) acetyl acetate resulting in an increase of CO conversion compared to that of cobalt nitrate (Kraum and Baerns, 1999). Disadvantages of cobalt catalysts are the high costs of cobalt and low water-gas shift activity.

3.6 Iron (Kittel, 1956; Pauling, 1988)

3.6.1 General

Iron is a chemical element with the symbol Fe (Latin: *ferrum*) and atomic number 26. Iron is a group 8 and period 4 metal. Iron is a lustrous, silvery soft metal. Iron and nickel are notable for being the final elements produced by stellar nucleosynthesis, and thus the heaviest elements which do not require a supernova or similarly cataclysmic event for formation. Iron and nickel are therefore the most abundant metals in metallic meteorites and in the dense-metal cores of planets such as Earth.

3.6.2 Physical Properties

Iron is a shiny, bright white metal that is soft, malleable, ductile and strong. Its surface is usually discolored by corrosion, since it combines readily with the oxygen of the air in the presence of moisture. In absolutely dry air, it does not rust. The oxide that is produced is crumbly and soft, giving no protection to the base metal, which eventually rusts away. It is found in nature as the metal only in meteorites and in very rare circumstances where iron minerals have been reduced by environmental factors. Masses up to 25 tons in weight have been found in West Greenland. Practically, it is always obtained from ores that are usually the oxides, and occasionally the carbonate, as low in sulphur and phosphorus as possible. The plentiful iron pyrite, FeS_2 is not an

acceptable ore because sulphur is a deleterious impurity in iron, and expensive to remove in refining. Iron is the fourth most plentiful element in the earth's crust (4.6%), but is so widely disseminated that it can be obtained only from ores in which iron has been specially concentrated. Much of this concentration, incidentally, occurred very early in the earth's history when iron removed from the atmosphere the little oxygen that it then contained, possibly with the help of the earliest forms of life.

Iron has atomic number 26, atomic weight 55.85, and stable isotopes 54 (5.9%), 56 (91.6%), 57 (2.2%) and 58 (0.33%). Its electron configuration is $Ar3d^64s^2$, and its first and second ionization potentials are 7.87V and 16.18V. With its neighbors cobalt (Z=27) and nickel (Z=28), it is one of the "iron triad" of similar metals. It is in the center of the periodic table, in the region of "transition metals" where a d-shell of electrons is being filled. The 4s electrons are actually more stable than the 3d electrons, so the d-electrons are actually on the outside of the atom. The d-shell can hold 10 electrons, and as it becomes nearly filled, drops below the 4s electrons in energy. All these atoms filling d-shells make metals that are very much alike; if the d-electrons were more inside, these metals would be even more alike than they are. More will be said in connection with magnetism, in which these electrons play leading roles.

At room temperature, iron is in the form of *ferrite*, or α-iron, a body-centered cubic structure. The density of α-iron is 7.86 g/cc. At 910°C it changes to γ-iron, which is face-centered cubic and somewhat softer. At 1535°C iron melts, and boils at 3000°C. Cobalt melts at 1480°C, nickel at 1455°C. The specific heat of any of the three metals is about 0.107 cal/g-K. The thermal conductivities of Fe, Co and Ni are 3.37, 3.81 and 4.19 cal/s-cm-K. Their electrical resistivities are 9.71, 6.24 and 6.84 μΩ-cm. These are "worse" than those of copper by factors of only 4 to 6, so the iron metals are very good conductors of electricity and heat. Comparing the numbers shows how similar these metals are in their physical properties. It has not heard whether cobalt and nickel make useful alloys with carbon, as iron does. They are much too expensive to use as structural metals, other than as alloying elements or coatings.

Iron occurs as the cations Fe^{++}, ferrous iron, and Fe^{+++}, ferric iron. Nickel and cobalt occur mainly as the dipositive ions, nickelous and cobaltous, but also in other oxidation states, usually in unstable compounds. A large number of important salts are formed with various anions. Fe^{++} will gladly donate an electron in an acid solution or in the presence of oxygen, so it is a reducing agent, oxidizing itself to Fe^{+++}. In alkaline solution, this ion will gladly accept an electron, so it is an oxidizing agent, reducing itself to the ferrous state. In acid solution, Fe will reduce H_+ to H_2, since its electrode potential is -0.44V, well above hydrogen's. Iron is, in fact, an active element.

Normally, the iron oxides are ferrous oxide, FeO and ferric oxide, Fe_2O_3. Ferrous oxide is not stable against partial oxidation to $Fe(II)(Fe(III)_2O_4)$, usually written Fe_3O_4 or $FeO{\cdot}Fe_2O_3$. This hard, black substance is *magnetite*, an important ore of iron and a very interesting substance in its own right.

3.7 Fe catalysts

Iron catalysts are commonly used because of their low costs in comparison to other active metals. An important advantage of iron over cobalt is that it is imparts great flexibility to the Fischer-Tropsch process. By variation in catalyst composition, method of preparation, method of reduction, composition of synthesis gas, and process conditions, the course of the reduction can be regulated for the production of a large fraction of wax, or gasoline, or olefins, or alcohols. In addition, iron is easily available from many sources, whereas the supply of cobalt is limited (Storch *et al.*). Most early FTS catalysts were prepared with precipitation techniques. Novel catalyst preparation methods sinter and fuse metal oxides with desired promoters. Alkali-promoted iron catalysts have been applied industrially for the Fischer–Tropsch synthesis for many years (Rao *et al.*, 1992). These catalysts have a high water–gas shift activity and high selectivity to olefins and appear to be stable when synthesis gas with a high H_2/CO ratio is converted (Jager and Espinoza, 1995).

3.8 Copper promoter in FTS

Because addition of difficulty reducible oxides and deposition of the catalyst oxides on certain carriers did not result in improved hydrocarbon productivity, the effect of copper oxide was studied. Copper has a high heat conductivity and yet does not induce methane production. It was thought that the presence of copper lowers the temperature required for reduction of the catalyst oxides. Copper somewhat enhance the activity of iron and cobalt, but not nickel. This was explained by Fischer on the basic of the tendency of nickel to form alloys with copper (Storch *et al.*).